Surface Science 604 (2010) 404–408

Contents lists available at ScienceDirect

Surface Science

journal homepage: www.elsevier.com/locate/susc

# Kinetic Monte Carlo simulation of the growth of metal clusters on regular array of defects on insulator

G. Sitja [a,*], R. Omar Uñac [b], C.R. Henry [a]

[a] Centre Interdisplinaire de Nanoscience de Marseille, UPR-CNRS 3118 Associated to Aix-Marseille Université, Campus de Luminy case 913, 13288 Marseille Cedex 09, France
[b] Instituto de Física Aplicada, Universidad Nacional de San Luis – CONICET – Ejército de los Andes 950, D5700HHW, San Luis, Argentina

ARTICLE INFO

*Article history:*
Received 2 September 2009
Accepted for publication 27 November 2009
Available online 11 December 2009

*Keywords:*
Nucleation
Growth
Surface diffusion
Palladium
Aluminium oxide
Monte Carlo simulation
Cluster arrays
Metal

ABSTRACT

A Kinetic Monte Carlo simulation of the nucleation and growth of Pd clusters on a nanostructured alumina substrate is presented. The new Monte Carlo simulation program allows to derive the 3D shape of the growing clusters without performing a full all atoms simulation. The simulation shows, like in previous pure 2D simulations, that clusters nucleate exclusively on the defects of the nanostructure in a limited range of substrate temperature. Around 300 K, the clusters have a compact faceted shape and they grow, at not too large coverage, layer by layer. These results are in agreement with previous studies of the nucleation and growth of Pd clusters on an ultrathin alumina film on $Ni_3Al$ (1 1 1).



## 1. Introduction

Metal clusters grown on oxide surfaces are important in several fields and especially as model catalysts [1–4]. As catalytic properties depend on the size of the particles [5] and on their shape [6] it is important to control the nucleation and growth kinetics of metal clusters on a surface by atom deposition. The nucleation on oxide substrates is strongly influenced by surfaces defects as on MgO [7,8] and $TiO_2$ [9]. The nucleation kinetics on point defects is relatively well understood through atomistic theory and mean field approach of the diffusion problem [7,10]. Another approach is to use Monte Carlo simulation that treats local variation of the density of adatoms [11].

In general the point defects are randomly distributed and the growth rate of the clusters is non-uniform that leads to fairly large size distributions [2]. A way to obtain sharp size distributions is to nucleate the clusters on a regular array of defects which allows a uniform growth rate of the clusters [12]. Such goal has been obtained, until recently, only on metals [13,14]. However since the discovery of nanopatterned oxide thin films, like alumina on $Ni_3Al$ (1 1 1) [15] or TiOx on Pt (1 1 1) [16], regular arrays of metallic and bimetallic clusters can be obtained [17–21]. These regular arrays of metal clusters present a very sharp size distribution decoupled of the density of clusters which is fixed by the density of the defects forming the nanostructure of the substrate. These systems represent quasi-ideal model catalysts on which intrinsic size effects can be studied conveniently [22]. However it is important to understand how nucleation and growth occurs on these systems.

Nucleation and growth kinetics of clusters on a homogeneous substrate [1,12,23] and on a regular array of clusters have been studied by Kinetic Monte Carlo simulations [24,25]. However previous studies concerned irreversible or 2D growth. In this paper we simulate by a Kinetic Monte Carlo method the nucleation and growth of Pd clusters on a nanopatterned alumina substrate, allowing nucleation, 3D growth and ripening.

## 2. Simulation method

A new simulation code has been developed which is based on the BKL (Bortz, Kalos, Lebowitz) Monte Carlo algorithm [26]. The model simulates the nucleation and growth on a hexagonal lattice which contains a hexagonal lattice of defects. On the defects the adsorption energy of an adatom is a little larger than on regular sites. In the model the defects can be really punctual (one atom large) or extended by a modulation of the adsorption energy which corresponds more to a periodic deformation of the substrate due to the strain in the film resulting from the misfit between the oxide ultrathin film and the metal substrate, as it has been suggested by atomically resolved AFM images of alumina films on $Ni_3Al$

* Corresponding author. Tel.: +33 06 60 36 28 29; fax: +33 04 91 41 89 16.
*E-mail address:* sitja@cinam.univ-mrs.fr (G. Sitja).

0039-6028/$ - see front matter © 2009 Elsevier B.V. All rights reserved.
doi:10.1016/j.susc.2009.11.037

(1 1 1) [27]. The main features of the simulation code are the following: periodic boundary conditions, 3D growth, calculation of the diffusion barriers by a broken bond model, possible reevaporation of adatoms, allowance of the calculation of a GISAXS image resulting from the cluster spatial distribution [22,28], output of the cluster density and statistical distributions (size, height, ...) which can directly be compared to experimental data.

In the Kinetic Monte Carlo method, all the possible elementary events and their probability of occurrence are examined at each calculation step. The evolution probability of the system, at a given time (i.e. in a particular configuration), corresponds to the sum of the probabilities of all the possible elementary events. In the case of the growth on a hexagonal lattice, for each occupied site, eight events are possible: an adatom can diffuse in six directions, it can desorb to the gas phase or an atom from the gas phase can be adsorbed on top of the considered adatom. For the unoccupied sites the only possibility is the adsorption of an atom.

The activation energies corresponding to individual events like desorption or diffusion are calculated and the probability $p_{ijk}$ ($i$ and $j$ correspond to the atomic position and $k$ to the considered type of event) for the event to be realized is calculated.

The global probability $P_g$:

$$P_g = \Sigma_{ijk} p_{ijk} \quad (1)$$

that a new event happens is inversely proportional to the average elapsed time for an event to occur. At every calculation step, the time is incremented by a value $1/P_g$ and a random number between 0 and $P_g$ is generated to determine the type of event and its location. The information on the different layer levels is given by the total number of atoms on the considered site. It is not a true 3D growth which would involve a 3D lattice of atomic sites but the rather 'phenomenological' approach followed here allows to correctly model the aspect ratio of the clusters (height/lateral size) keeping the speed of a pure 2D simulation.

To be more precise, a 2D array $T(i, j)$ of integer is used to represent the state of the system at a given time. Each array element contains the number of atoms situated on top the site $i,j$ of the substrate. $T(i, j)$ can take any positive value and is equal to 0 when there is a bare site at the considered place. When considering an eventual diffusion from an atom at the position $i, j$, the environment of the atom in the same layer and in the under and upper layers are taken into account. In the same layer, the atom at position $i, j$ interacts with (if they exists) the atoms at positions $i, j-1$; $i, j+1$; $i-1, j$; $i+1, j$ and, to represent correctly an hexagonal array on a (1 1 1) surface, with atoms at position $i+1, j+1$ and $i-1, j-1$.

Interactions with neighbouring layers follow the same interaction rules plus interaction at the same position (i.e. $i, j$) with the underlayer. An isolated adatom is then in interaction with seven atoms in the underlayer. This allows to set independently adsorption energy and diffusion energy.

When having more than one atom at position $i, j$, (i.e. $T(i, j) > 1$) we consider that only the top atom can move.

The energy barrier is calculated taking into account for the modification (breaking) of considered bounds. We allow every movement except long jumps (not considered) and crossing up steps that are higher than one layer high (setting a very high energy barrier for those events). Fig. 1 illustrates in one-dimension various kinds of allowed movements and the interactions taken into account to calculate the energy barrier. As shown in Fig. 1e and f, an adatom on top of a step will have a huge probability to diffuse on the terrace because this movement requires to break very few bonds. This implies that having an adatom on top of a step is very seldom encountered during calculations. This effect is comparable to that we expect when a Schwoebel barrier is considered, promoting the growth of particles layer per layer. Although the equilibrium shape of clusters would be a hexagonal truncated pyramid, with the height/diameter ratio determined by the adsorption energies used in the calculations, in our simulation, growth can exhibit many different behaviours depending on the temperature, deposition rate, and the energies included in the system (i.e. the two adsorption energies and the two diffusion energies). However, as the model is an enhanced 2D model and not a 3D model, it is impossible to observe contact angles larger than 90°.

An array 2D of float $S(i, j)$ contains the information of the total binding energy for a metal atom on the substrate at the place $i, j$. This array is used only for atoms directly in contact with the substrate.

The probability of occurrence $P_o$ of a given event is obtained by calculating the probability that the energy of the considered atom, at a given time, would be higher than the activation energy of this event. If we assume that the energy distribution of the atoms follows the Boltzmann law, at a temperature $T$, the probability to have a given atom with an energy above a limit $E$ is $P = \exp(-E/kT)$. The atom attempt to move $v$ times per second (this frequency is set to $10^{13}$ Hz), thus the probability of occurrence $P_o$ for an event requiring $E_{event}$ is $P_o = v \cdot \exp(-E_{event}/kT)$.

For the simulation in this work, a 2D grid with $200 \times 200$ sites is considered. The energies involved in the simulation which corresponds to the breaking of the metal–metal and metal substrate bonds are adjusted in order that the global metal–metal bond corresponds to experimental Pd–Pd bond, the adsorption energy of a Pd atom on a Pd facet is taken equal to 1.086 eV. A DFT calculation gives a value of 1.5 eV [29] and from the cohesion energy one estimates a value of 0.98 eV. The diffusion energies of Pd/Pd (1 1 1) facets is set to 0.471 eV. The mean adsorption energy of a Pd atom on the substrate has been set to 1.146 to correspond to the experimental value of the adhesion energy of $Pd/Al_2O_3$ film [30].

In fact, it is not clear if the observed organization of the clusters [17–21] is due to point defects or to a modulation of energies (diffusion or/and adsorption) on the substrate. As it is obvious that we can get organization with point defects, we have chosen to focus on the case of a modulation of the metal substrate adsorption energy instead of point defects. The modulation amplitude is set to 10% (thus, the diffusion energy of a Pd atom on the substrate varies from 0.447 to 0.546). In the following, we will call "defects" the sites of maximum diffusion energy (Pd-substrate).

## 3. Results

The calculations have been made in order to simulate the nucleation and growth of Pd clusters on a nanostructured alumina with an hexagonal lattice of defects separated by 20 atomic sites that corresponds to the dot structure of the alumina ultrathin films on $Ni_3Al$ (1 1 1) with a distance of 4.1 nm between the defect sites [27]. The substrate temperature has been varied from 190 K to 400 K and the Pd flux from 0.01 to 10 ML/s. The Pd coverage was limited to 0.1 ML in almost all simulations.

Fig. 2 presents a series of simulation snapshots corresponding to increasing deposition times at 300 K and for a deposition rate of 1 ML/s. We see that the density of clusters increases rapidly and reaches saturation where the clusters occupy all the nodes (i.e. the defects) of the nanostructure.

Fig. 3 shows a series of nucleation kinetics at 300 K with increasing fluxes from 0.01 to 6.67 ML/s. We see that for large deposition rates, a maximum value of the density of clusters is rapidly reached (saturation density) which corresponds, at this temperature, to the density of defects. However, at the smallest deposition rates the nucleation frequency decreases (slope at the origin of the nucleation kinetics) and the saturation density of clus-

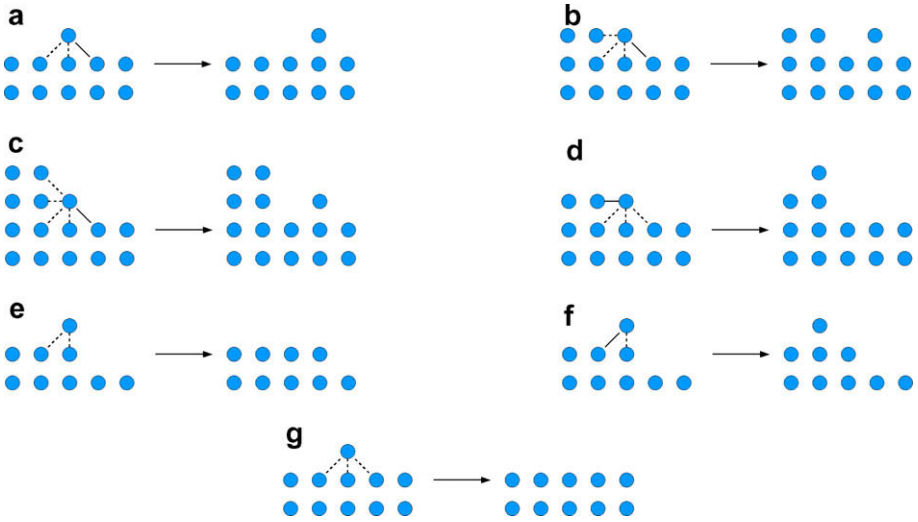


**Fig. 1.** Various kinds of possible movements. Dashed lines represent interactions taken into account for the considered movement: (a) diffusion, (b) detachment from a step, (c) detachment from a 3D edge, (d) crossing a step toward an upper layer, (e) diffusing from an edge to a terrace, (f) falling down from a terrace and (g) desorption.

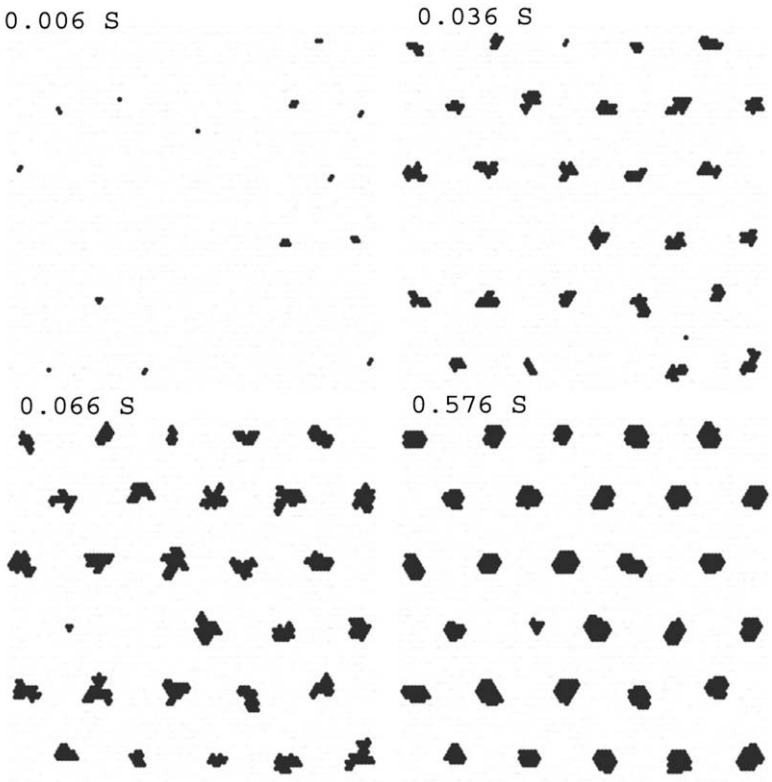


**Fig. 2.** Series of simulation snapshots at 300 K and for a deposition rate of 1 ML/s, corresponding to increasing times: 0.006, 0.036, 0.066 and 0.576 s.

ters is not reached at the maximum coverage (0.1 ML) considered in the simulation.

Fig. 4 displays the saturation density of the clusters as a function of the substrate temperature in an Arrhenius plot at a deposition rate of 0.5 ML/s. We see that between 230 and 300 K, all the defects and only them are occupied by the clusters. This means that the diffusion length of the adatoms is larger than the distance between two neighbouring defect sites. At low temperature the diffusion length is shorter and two adatoms can meet each other before to reach a defect sites, then homogeneous nucleation occurs in addition to heterogeneous nucleation and the maximum density of clusters increases with decreasing temperature. In the Arrhenius plot (Fig. 4) this part of the curve is linear and then an activation energy of 0.210 eV is obtained. From nucleation theory on defects one expects, for a random distribution of defects, an activation energy in the low temperature regime equal to 1/3 of the diffusion energy [10,25]. In our simulation this would corresponds to 0.166 eV. Which is a little smaller than the measured value.

In the high temperature range a straight line can be also determined which corresponds to apparent activation energy of 0.118 eV. However the accuracy of this determination is low because of the limited number of points corresponding to the high temperature domain due to the prohibitive simulation times.

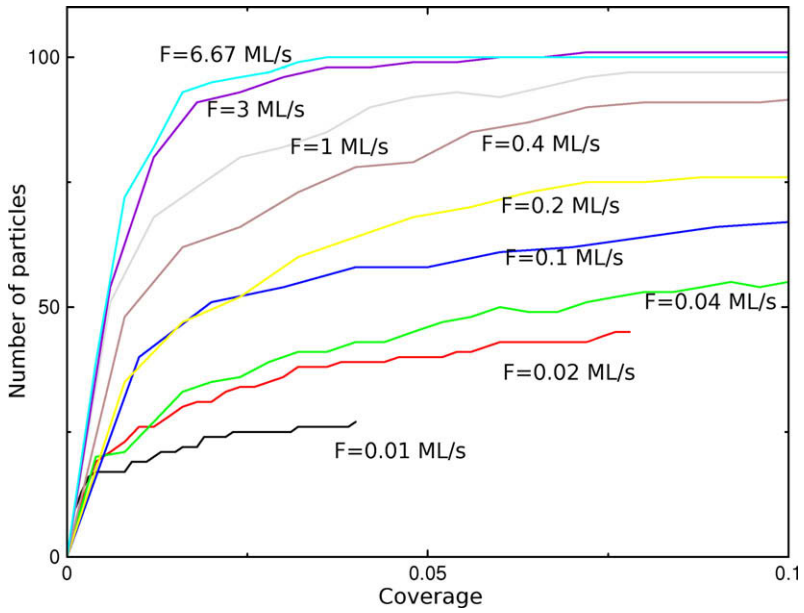


**Fig. 3.** Nucleation kinetics for various deposition rates at 300 K. The maximum number of particles (100) corresponds to the number of defects on the simulation grid.

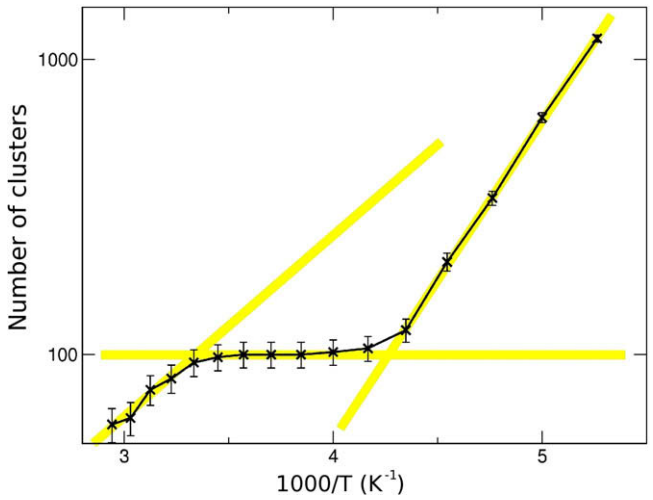


**Fig. 4.** Arrhenius plot of the saturation density of clusters as a function of the reciprocal substrate temperature. The errors bars correspond to statistical fluctuations. The coloured straight lines correspond to limiting cases of pure nucleation on defects (intermediate temperature range), imperfect nucleation on defects (high temperature) and homogeneous nucleation (low temperature). (For interpretation of the references to colour in this figure legend, the reader is referred to the web version of this article.)

At high temperature all the defects are not filled by clusters. This is due to the fact that, at these temperatures, adatoms trapped on the defects can escape and be captured by clusters nucleated on another defect, the defects are no longer perfect sinks for adatoms.

Fig. 5 displays a series of snapshots corresponding to different substrate temperatures. At low temperatures the clusters are ramified because the diffusion of Pd atoms at the edge is not sufficiently fast compared to the arrival rate of adatoms to form compact islands. At 300 K the clusters are thicker and they have a compact hexagonal shape. A detailed analysis of the evolution of the shape of the clusters shows that at 300 K, below a coverage of 0.1 ML, the clusters grow layer by layer (i.e. the $n+1$ layer starts to grow when the $n$ layer is complete).

This result is in agreement with the histograms of height obtained by STM for the growth of Pd clusters on alumina on $Ni_3Al$ (1 1 1) which shows only sharps peaks corresponding to successive atomic layers [21].

The size distribution is rather sharp and becomes thinner at higher temperature. Fig. 6 shows a snapshot corresponding to growth at 300 K and for a flux of 10 ML/s. The size histogram shows a mean size of 5.3 interatomic distances and a size dispersion of 7.3%. The average number of atoms is 39.7 with a dispersion of 19% which is only 1.44 larger than the smallest possible dispersion.

## 4. Discussion

The Kinetic Monte Carlo simulations presented here, show qualitatively the same nucleation kinetics as for the growth of metal clusters on a random distribution of defects like for Pd/MgO (1 0 0) [7,11] except that the low temperature limit was not reached in those experiments. In the simulation of the 2D growth of Co islands on a nanostructured gold surface [25], the three temperature domains, like in Fig. 3, appeared in experiments and in the simulations. The main advantage of the present simulations is to have information about the 3D-shape of the clusters.

If we compare the present simulation with the experiments on the growth of Pd clusters on nanostructured alumina ultrathin films on $Ni_3Al$ (1 1 1) [17,18,21], there is a good agreement. At room temperature we are in the optimum condition where nucleation occurs only on the defects of the nanostructure that leads to well organized arrays of clusters. In the case of gold we never cover all the defects sites at room temperature which probably means that the Au/alumina interaction is weaker than in the case of Pd, then gold atoms or tiny clusters can escape from the defects [21]. Our simulations show that in the case of gold, room temperature probably corresponds to the high temperature region of Fig. 4, where all clusters are on defect sites but where all defect sites are not covered. It is important to notice that the domain of perfect nucleation on defects (all particles are on defects and all defects are occupied) depends of the considered metal/substrate system. A way to circumvent this problem is to nucleate a few atom cluster on each defect and then to grow another metal that normally does not present perfect nucleation on defects. This has been already used to grow a lattice of gold [18] and Fe [20] nanoparticles using

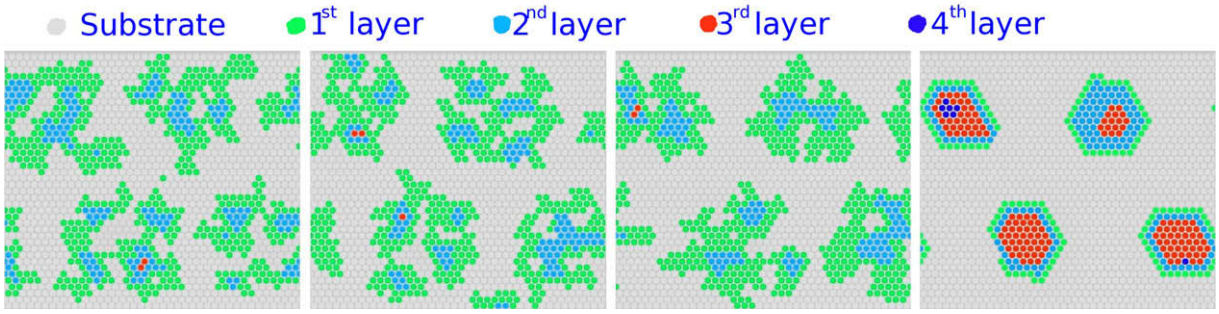


**Fig. 5.** Series of simulation snapshots (part of the images) corresponding to the growth of Pd clusters at increasing substrate temperatures: from left to right 220, 230, 240 and 300 K. The deposition rate and time are 0.1 ML/s and 5 s, respectively.

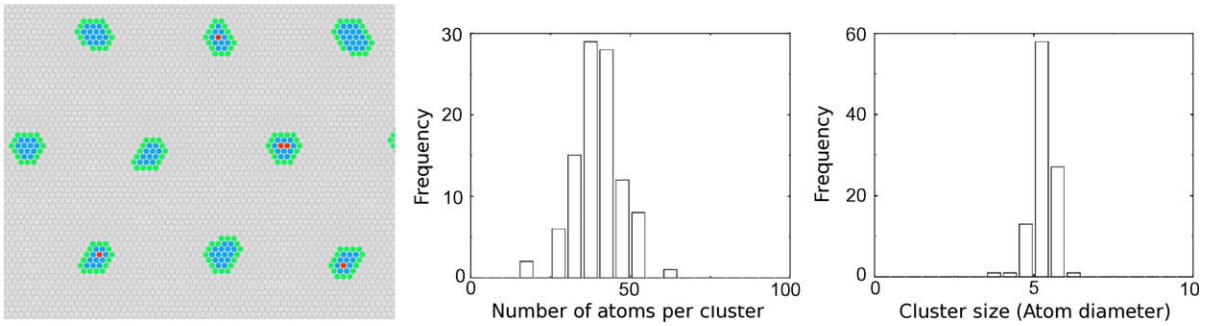


**Fig. 6.** Part of a simulation snapshot corresponding to the growth of Pd clusters at 300 K for a deposition rate of 10 ML/s and a deposition time of 0.01 s of deposition (Same colour code than Fig. 5). On the right the distributions of number of atoms per clusters and of the cluster size are represented.

Pd clusters as a seed. The size distribution of the clusters is very narrow in the simulation but it cannot be directly compared with experiments because the effect of the STM tip-cluster convolution enlarges the clusters especially for smaller ones. However, the experimental height distribution [21] are very precise and in good agreement with the layer by layer growth mechanism which is observed in the simulations at 300 K. A compact cluster shape is also observed experimentally by STM [17,18,21,22] at room temperature. This result demonstrates that already at room temperature surface self diffusion is active on the Pd clusters. It is interesting to note that with a modulation of the diffusion energy by only ±10% (the maximum value being on the defects) one obtains a good organization of the clusters while with a lattice of point defects a much higher adsorption energy is required.

## 5. Summary and conclusion

In this paper we have presented a new Kinetic Monte Carlo model that is able to simulate the nucleation and the 3D growth of metal clusters on a nanostructured surface. These simulations adapted to the case of Pd on a nanostructured alumina thin films give good agreement with previous STM studies of the growth at room temperature of regular arrays of Pd clusters on an ultrathin film on $Ni_3Al$ (1 1 1). Very quickly all the defects sites are occupied and no homogeneous nucleation occurs. At 300 K the clusters grow in a compact shape with a layer by layer mechanism and a narrow size dispersion (around 7%). Further simulations with the same model are undertaken to study the stability of the cluster organization after annealing at high temperature.

## References

[1] C.T. Campbell, Surf. Sci. Rep. 27 (1997) 1.
[2] C.R. Henry, Surf. Sci. Rep. 31 (1998) 231.
[3] H.J. Freund, Catal. Today 100 (2005) 3.
[4] A.K. Santra, D.W. Goodman, J. Phys. Condens. Matter 14 (2002) R31.
[5] M. Che, C.O. Benett, Adv. Catal. 36 (1989) 55.
[6] C.R. Henry, Prog. Surf. Sci. 80 (2005) 92.
[7] G. Haas, A. Menck, H. Brune, J.V. Barth, J.A. Venables, K. Kern, Phys. Rev. B 61 (2000) 11105.
[8] C. Barth, C.R. Henry, Phys. Rev. Lett. 91 (2003) 196102.
[9] N. Lopez, R. Schaub, P. Thostrup, A. Ronnau, C. Africh, E. Laegsgaard, J.K. Norskov, F. Besenbacher, Phys. Rev. Lett. 90 (2003) 026101.
[10] J.A. Venables, J.H. Harding, J. Cryst. Growth 211 (2000) 27.
[11] L. Xu, C.T. Campbell, H. Jonsson, G. Henkelman, Surf. Sci. 601 (2007) 3133.
[12] H. Brune, Surf. Sci. Rep. 31 (1998) 121.
[13] H. Brune, M. Giovannini, K. Broman, K. Kern, Nature 394 (1998) 451.
[14] H. Ellmer, V. Repain, M. Sotto, S. Rousset, Surf. Sci. 511 (2002) 183.
[15] A. Rosenhahn, J. Schneider, C. Becker, K. Wandelt, J. Vac. Sci. Technol. A18 (2000) 1923.
[16] F. Sedona, S. Agnoli, M. Fanetti, I. Kholomanov, E. Cavaliere, L. Gavioli, G. Granozzi, J. Phys. Chem. C111 (2007) 8024.
[17] S. Degen, C. Becker, K. Wandelt, Faraday Discuss. 125 (2003) 343.
[18] G. Hamm, C. Becker, C.R. Henry, Nanotechnology 17 (2006) 1973.
[19] A. Lehnert, A. Krupski, S. Degen, K. Franke, R. Decker, S. Rusponi, M. Kralj, C. Becker, H. Brune, K. Wandelt, Surf. Sci. 600 (2006) 1804.
[20] M. Schmid, G. Kresse, A. Buchsbaum, E. Napetschnig, S. Gritschneder, M. Reichling, P. Varga, Phys. Rev. Lett. 99 (2007) 196104.
[21] M. Marsault, G. Hamm, A. Wörz, G. Sitja, C. Barth, C.R. Henry, Faraday Discuss. 138 (2008) 407.
[22] G. Hamm, G. Sitja, F. Leroy, M. Marsault, G. Renaud, C.R. Henry, submitted for publication.
[23] T.A. Witten, L.M. Sander, Phys. Chem. Lett. 47 (1981) 1400.
[24] C. Lee, A.L. Barabasi, Appl. Phys. Lett. 73 (1998) 2651.
[25] S. Rohart, G. Baudot, V. Repain, Y. Girard, S. Rousset, H. Bulou, C. Goyhenex, L. Proville, Surf. Sci. 559 (2004) 47.
[26] A.B. Bortz, M.H. Kalos, J.L. Lebowitz, J. Comput. Phys. 17 (1975) 10.
[27] G. Hamm, C. Barth, C. Becker, K. Wandelt, C.R. Henry, Phys. Rev. Lett. 97 (2006) 126106.
[28] G. Renaud, R. Lazzari, C. Revenant, A. Barbier, M. Noblet, O. Ullrich, F. Leroy, Y. Borensztein, J. Jupille, C.R. Henry, J.P. Deville, F. Scheurer, J. Mane-Mane, O. Fruchart, Science 300 (2003) 1416.
[29] A. Bogicevic, D.R. Jennisson, Phys. Rev. Lett. 82 (1999) 4050.
[30] K. Højrup-Hansen, T. Worren, S. Stempel, E. Laegsgaard, M. Bäumer, H.J. Freund, F. Besenbacher, I. Stensgaard, Phys. Rev. Lett. 83 (1999) 4120.